Energy 175 (2019) 667–676

Contents lists available at ScienceDirect

Energy

journal homepage: www.elsevier.com/locate/energy

Effect of different flow schemes on heat recovery from Enhanced Geothermal Systems (EGS)

Pranay Asai, Palash Panja, John McLennan, Milind Deo*

Department of Chemical Engineering, University of Utah, United States

ARTICLE INFO

Article history:
Received 3 October 2018
Received in revised form
19 March 2019
Accepted 22 March 2019
Available online 23 March 2019

Keywords:
Enhanced geothermal system (EGS)
Flow scheme comparison
Operational optimization
Doublet well system
Instantaneous power
Total heat recovery

ABSTRACT

Operational optimization is the key to maximize the heat extraction efficiency of Enhanced Geothermal Systems (EGS). Injection/production flowrate is one of the operational parameters that can be easily manipulated to produce desired amount of energy. In this study, the effect of different flow schemes on the rate of heat production is analyzed over a period of 30 years. Seven flow schemes (four continuous functions namely constant flow, linear flow, exponential flow, mirror exponential flow, and three step functions with step sizes of six months, three years and ten years) developed on the basis of mathematical functions were examined. A doublet EGS model with a single fracture was simulated using a commercial thermal reservoir simulator. The reservoir and well data were obtained from the FORGE (Frontier Observatory for Research in Geothermal Energy) site at Milford Utah. The results were analyzed on the basis of their temperature decline curves for the produced water and the total amount of heat extracted over the entire period. The exponential flow scheme is the optimum case considering the rise in energy demand over the next 30 years. The amount of heat extracted per unit volume of water decreases with increase in total water volume circulated.

© 2019 Published by Elsevier Ltd.

1. Introduction

The search for a sustainable, renewable and a clean source of energy is something that humans have longed for since the development of modern society. One such source of energy which has potential to meet all the three criteria lies just beneath our feet, the geothermal energy. Geothermal energy can be harnessed from the hot dry rock (HDR) that lies deep inside the Earth's crust. HDR has been a tempting field of interest since the early 1970s and so far many different technologies have been developed to commercialize this form of energy [1–3]. Over the last decade one such technology that looks promising to harness the heat has surfaced, that is Enhanced Geothermal Systems (EGS) [4]. An EGS consists of two or more well system which are connected by naturally occurring or artificially created fractures to facilitate a flow of a fluid in the system. A simple EGS would consist of an injection well, a production well and one or multiple fractures connecting the two wells along its length. Then a carrier fluid with high heat capacity is circulated in the system to bring the subsurface heat over to the surface of the earth. This hot fluid can then be used to run the turbines and generate electricity.

Though as simple as it may seem, developing a working EGS poses several major challenges. The efficiency of an EGS mainly depends on the temperature of the produced fluid which in turn depends on the temperature of the reservoir. The subsurface temperature increases as we go deep in the Earth's surface. Creating an interconnected system of wells 8000–10000 feet below the Earth's surface is no easy task. Though this can be made possible through the well drilling knowledge acquired from oil and gas industry, it would still require large capital investments. Unlike Oil and Gas formations, an optimum EGS reservoir would have high density, low porosity (this leads to high heat capacity) and higher temperatures, which makes the drilling process difficult and even more expensive [5]. Li and Lior [6] calculated that the amount of energy spent developing an EGS could go as high as 19.40 $TJ/(km\ of\ well)$. But when the drilling methods are optimized it could result in high energy return on investment (EROI) of 33.8–286.2 for the EGS.

Many recent studies that have been conducted to optimize the EGS have mainly focused on effects of various completion and operational parameters. Wu et al. [7] developed a simplified model for an EGS to circulate fluid in a closed loop for heat extraction. Frash et al. [8] evaluated doublet and triplet well systems to show

* Corresponding author.
E-mail address: milind.deo@utah.edu (M. Deo).

https://doi.org/10.1016/j.energy.2019.03.124
0360-5442/© 2019 Published by Elsevier Ltd.

the importance of well trajectories and the need for proper intercepts with the fractures to ensure the flow. Chen et al. [9] performed a comparative performance studies on the doublet, triplet and quintuplet well layout. They concluded that the doublet well layout is the most effective way for HDR energy exploitation. Researchers have compared the effects of coupled processes (thermo-hydro versus thermo-hydro-mechanical), operational parameters and reservoir parameters on heat recovery from EGS [10–12]. They showed that coupling has significant impacts on the estimation of heat extraction. Vazquez-Rubio et al. [13] compared various simulation codes developed by universities, research centers and national laboratories to model the fracture responses to Thermal-Hydrology-Mechanical (T-H-M) factors in engineered geothermal systems. Two cases were studied; a poroelastic fault layer in a geothermal reservoir with water injection and a single planar fracture in hot rock.

Sanyal et al. [14] evaluated the effect of completion parameters by studying five-spot layout model (hypothetical) with fracture spacing and well geometry. Aliyu et al. [15] showed that the reservoir parameters have a dominant effect on heat production to the human controlled parameters (operational parameters). Their model was based on Soultz (France) geothermal field but they only used a constant flow rate of 10 l/s in this study. Sun et al. [16] showed how different discreet fracture models affect the heat extraction in the reservoir. Xia et al. [17] showed how the well inclination and fluid flow rate affects the power generation form an EGS. They used two different injection rate (constant) to show the comparison. Zeng et al. [18] investigated the performance of a single facture at Desert Peak field with constant flow. They concluded that the desired efficiency for the system could be obtained from large fracture width to ensure high flow rate. Asai et al. [19] showed the combined effect of the completion and operational parameters on the heat production.

Even though some of these designs can be highly efficient in developing an economical system, there is still one major problem to address, the growing demand of energy with time. As the heat energy from the EGS reservoir is extracted, the in-situ temperature of the reservoir drops because the rate of heat transfer from the Earth's subsurface to replenish the reservoir is slower than the rate of heat extraction. This means that over time the power output of the geothermal plant will decrease, which is counterintuitive to the rise in energy demand over the same time. This means either more EGS systems have to be installed over time or would have to rely on another source of energy to balance this decline.

1.1. Rise in energy demand

In this ever-growing society, our dependence and need for energy is constantly increasing. U.S. Energy Information Administration (EIA) predicts a growth of 48% (Fig. 1) in energy consumption between 2012 and 2040 [20]. It also predicts that the renewable energy would be the fastest growing energy sources over the projection period. Most of our renewable energy today comes from hydropower, solar and wind [15]. Though these sources have proved to be quite efficient, they are still not reliable enough to match up the energy consumption throughout the day. Hydropower is mostly reliable but as there are limited streams of water, it is not available everywhere. Solar and wind are highly dependent on the climatic conditions and also on the location, and hence can't assure a continuous supply of power.

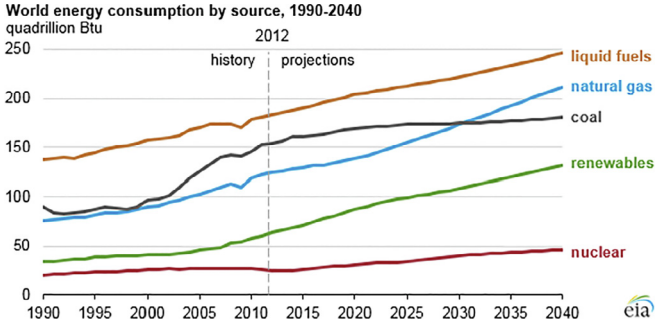

Fig. 1. World energy consumption by source, 1990–2040.

Here, geothermal energy would prove to be a better substitute as it has a potential to supply constant power throughout the day, similar to the output from fossil fuel or coal operated power plant. This can be easily done by manipulating the operational parameters to vary the output throughout the day. The operational parameters like injection/production flow rate are flexible enough and can be manipulated as needed. Hence geothermal energy would prove to be a more reliable source to match up the daily energy consumption. But is it capable of matching the demand over time, with increase in energy consumption over years? Can the output be increased, without installing additional EGS? Answering these questions by seeking sustainable operational schemes is the main focus of this research.

This study acknowledges these major challenges and proposes innovative way to match up the increase in energy demand by optimizing the operation of the EGS over its life. The objective of this study is to evaluate different flow (operating) schemes in the EGS and determine their effect on the decline of the reservoir temperature and power output.

2. Methodology

A series of simulations were performed by designing experiments based on variable flow schemes that can be potentially used in an EGS. When an EGS system is established, the rate at which the geothermal reservoir can be depleted is directly the function of the operational parameters [19]. The operational parameters that can be manipulated include, type of fluid to be circulated, injection temperature of the fluid and the flow rate of the injected/produced fluid. Out of these three, flow rate is the easiest on to manipulate so as to get the desired results. In this study the effects of different flow schemes were evaluated over the span of 30 years to see the effect on the total power output from an EGS.

Due to high temperature of the injection fluid (water), it tends to dissolve salts and other minerals, which may get deposited when the fluid cools down at the surface. This may result in scaling in the pipes and other parts of the plant. The dissolution of silica also aids in increasing fracture transmissivity in the longer run, as mentioned by Pandey et al. [21] and Gan et al. [22]. However, these effects are not considered in this study and it was assumed that the pure water was injected and produced from the reservoir.

2.1. Design of operational schemes

Seven different flow schemes were considered in this study. In four of the schemes, flow rates are varied continuously (continuous functions) with time and in three other schemes the rates are varied discreetly (step function) with time. The four continuous ones are constant flow rate (termed constant from here on), linearly increasing flow rate (linear), exponentially growing flow rate (exponential), and mirror of exponential flow rate with respect to the linear flow rate (bounded exponential). The three discrete flow schemes are six month step increment (6 months), three year step increment (3 years), and 10 year step increment (10 year).

To ensure all the cases are comparable, the total amount of fluid

circulated over 30 years was kept constant. Also, as all the cases except for constant flow rate have increase in flow with respect to time and the initial flow rate in these schemes was half of the flow rate in the constant flow model. This was done to ensure the total area under the curve (total fluid flow) was constant.

Initial conditions including injection temperature and fluid type (water in this case) were kept the same in all simulations. The equations representing the instantaneous flow rate for each individual scheme are shown below:

$$q(t) = a \tag{1}$$

$$\int_0^T q(t) = aT = C \tag{2}$$

Equation (1) represents the constant flow rate 'a' throughout the life of the well and equation (2) represents the cumulative flow over the period of 30 years (T).

Equation (3) represents the linearly increasing flow with time. As the initial flow for all the cases (except constant flow rate) is half of the constant flow rate, substituting that gives:

$$q(t) = \frac{a}{2} + bt \tag{3}$$

The cumulative flow can be represented as show in equation (4):

$$\int_0^T q(t) = \frac{a}{2}T + \frac{bT^2}{2} = C \tag{4}$$

Equation (5) represents the exponential increase of flow with time and equation (6) represents the cumulative water over 30 years in this flow scheme.

$$q(t) = \frac{a}{2}\exp(bt) \tag{5}$$

$$\int_0^T q(t) = \frac{a}{2b}[\exp(bT) - 1] = C \tag{6}$$

Equation (7) represents the mirror of exponential curve with respect to the linear curve and equation (8) represents the cumulative water injected over 30 years in this scheme.

$$q(t) = 2\left(\frac{a}{2} + b_1 t\right) - \frac{a}{2}\exp(b_2 t) \tag{7}$$

$$\int_0^T q(t) = \frac{a}{2}T + \frac{b_1 T^2}{2} - \frac{a}{2b_2}[\exp(b_2 T) - 1] = C \tag{8}$$

Equation (9) represents the instantaneous flow in a step function depending on the step size (6 months, 3 years and 10 years). This scheme forms an arithmetic series and hence the sum can be calculated as shown in equation (10) (sum of an arithmetic progression), which represents the cumulative water over 30 years. Here 't' represents the step size and 'T' is the total time (30 years), so the number of steps 'n' can be calculated as given in equation (11).

$$q(t) = \frac{a}{2} + \left[\frac{T}{t} - 1\right]b \tag{9}$$

$$\int_0^T q(t) = \sum_0^n q(t) = \frac{n}{2}[a + (n-1)b] = C \tag{10}$$

$$n = \frac{T}{t} \tag{11}$$

In all the above equations, 'b' represents the growth factor in each of the respective schemes and can be back-calculated as the total flow in the given time period of 30 years is known.

2.2. Design of experiments

The data for the flow rate was based on the study carried out by Xia et al. [17], which shows that the flow rate of 0.1 m^3/s for 40 fractures for 30 years or total of 2.37×10^6 $m^3/fracture$ yields maximum electric power output of 5 MW. In this study, the total amount of water of 2×10^6 $m^3/fracture$ was considered to be circulated in the EGS for 30 years. Using this the flow rate for the constant scheme is calculated and therefore for the other schemes as well. Also the growth factor (b) is calculated by using this information. The initial flow rate 'q_i' and the growth factor 'b' for all the flow scheme is shown in Table 1.

To make the study more robust, two more cases with different cumulative flow of water over 30 years were incorporated. Case 1 had total flow of 1.5×10^6 $m^3/fracture$ (Q1), case 2 had 2×10^6 $m^3/fracture$ (Q2) and case 3 had 2.5×10^6 $m^3/fracture$ (Q3). The various operating schemes for total flow for Case 2 are shown in Fig. 2. This was incorporated to visualize the effect of total fluid flow on heat extraction.

2.3. Doublet enhanced geothermal system

In this study a hypothetical doublet system was considered, consisting of one injection well and one production well drilled horizontally in a reservoir (Fig. 3). The two wells were assumed to be connected by '$\boldsymbol{n_f}$' (number of fractures) equally spaced and identical fractures. These fractures are developed and propagated by using various stimulating techniques which include hydraulic fracturing or by chemical stimulation as demonstrated by Luo et al. [23]. The fracture spacing was kept large enough to avoid any inter-fracture interactions. This was done so as to simplify the system and allow simulation of one fracture. The results could then be extended for the entire reservoir as in Asai et al. [24]. The simulated factures were assumed to be planar, rectangular, uniform and isotropic in nature. The heat transfer in fractures depends on the total surface area of the fracture; keeping the total surface of the simulated fracture the same would help apply results to fractures of other shapes [25]. The cooling effect of the reservoir may also lead to formation of additional fractures or preferential fluid paths, as

Table 1
The initial flow rare and growth factor for all the seven flow scheme for case 2.

Label	Flow Scheme	Flowrate (m^3/day)		
		Initial (q_i)	Growth (b) or (b_1 & b_2)	
Scheme 1	Constant	183	–	
Scheme 2	Linear	91.5	0.08326	
Scheme 3	Exponential	91.5	0.00011	
Scheme 4	Bounded	91.5	0.08326	0.00011
Scheme 5	6 months Step Up	91.5	3.15	
Scheme 6	3 years Step Up	91.5	27.92	
Scheme 7	10 years Step Up	91.5	73.03	

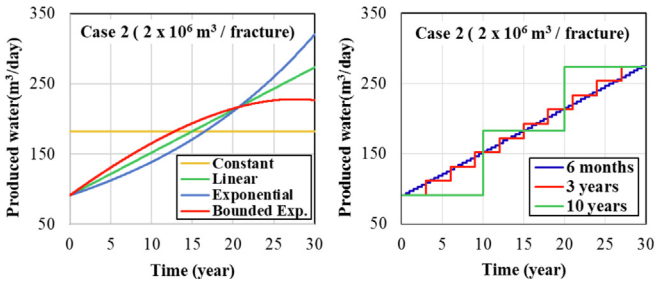

Fig. 2. Instantaneous flow rate in each individual scheme for Case 2. (a) Flow scheme for continuous function, (b) Flow scheme for step functions.

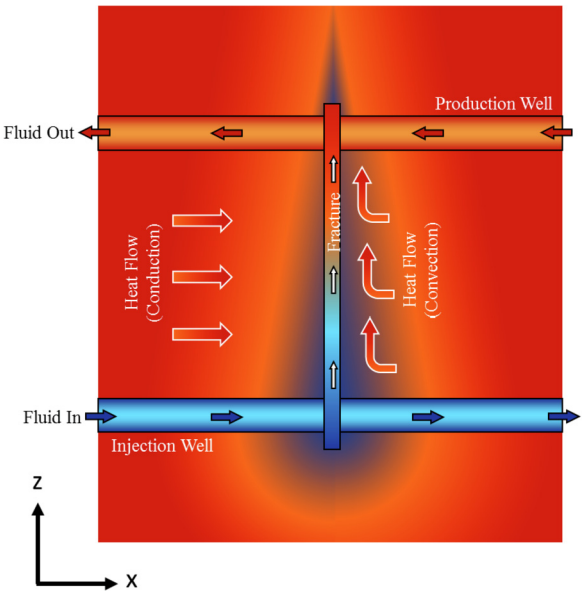

Fig. 3. Schematic representation of a heat transfer in the fracture and the reservoir.

mentioned by McDermott et al. [26]. To get around this (to keep the simulations simple), the average width of fracture over 30 years was calculated [20] to perform the simulation. In this study, geomechanical effects on fracture morphology were not considered.

The dimensions of the reservoir model for one fracture along with well dimension and fracture dimension are mentioned in Table 2. The dimension of the reservoir were adjusted according to the fracture size to ensure that the temperature at the boundaries remains unchanged at the end of 30 years [19,24].

The reservoir data for the simulation was obtained from the FORGE (Frontier Observatory for Research in Geothermal Energy) [27–29] site, situated in Milford, Utah. The granite formation at the FORGE site has low porosity of 1% and low permeability around $200\mu D$ to $1000\mu D$, situated at the depth of $2500m$. The temperature at this depth is around $200°C$ with a geothermal gradient of $60°C/km$, which makes it an optimum location to set up a geothermal system. The other reservoir properties of the FORGE reservoir are mentioned in Table 3. Because the porosity and permeability of the formation are insignificant as compared to the fractures, it is safe to assume that there is no fluid loss into the formation.

The combined design and reservoir data was then simulated using commercially available thermal reservoir simulator, CMG STARS. STARS, a reservoir simulator from Computer Modeling Group (CMG) based in Calgary Canada, can be used for performing simulations to interpret the heat and fluid transfer in a reservoir in given time. STARS is a three-phase, three-dimensional, multicomponent thermal simulator. It is widely accepted and used to perform studies on geothermal reservoirs and evaluate different possibilities [19,24,30–32]. It uses fully implicit and adaptive implicit methods for numerical solution of reservoir models with Cartesian, cylindrical, or variable depth/variable thickness grid systems.

Water is used as the heat carrier fluid in this case as it has high heat capacity, cheap and easily available. To produce heat from the system, water is injected at a decided injection temperature through the injection well where it reaches the reservoir and travels through the fractures where it gathers heat and its temperature increases and then is produced via production well. The produced water is then passed through a binary power plant where its enthalpy is transferred to the other fluid which runs the turbine and electricity is generated. Then the water is again pumped back through the injection well and the cycle continues. During the entire cycle, it is ensured that the water is pumped and produced at high enough pressure so that there is no phase change.

Using this simulation design and the flow scheme designed in earlier section, total of 21 simulations were run for all the seven schemes with three different total fluid flow. This analysis and the results were scaled-up to 50 fractures to get results for the whole system. The observation and results are discussed in the following section.

3. Results and discussions

It is observed that the temperature of the produced water declines with time. The temperature of the produced fluid depends on the temperature of the reservoir, residence time (flow rate) and the surface area (contact area) inside the fracture. The heat transfer

Table 2
Dimensions of reservoir model and fracture.

Well Properties	Dimension
Well Spacing, m	300
Fracture spacing, m	120
Well Inclination, degrees	90
Model Properties	
Reservoir length (X-direction), m	120
Reservoir width (Y-direction), m	440
Reservoir height (Z-direction), m	570
Fracture Properties	
Fracture width, m	0.01
Fracture half length, m	120
Fracture height, m	400

Table 3
Reservoir Properties of the FORGE site.

Properties	Value
Density of the rock, (kg/m^3)	2700
Permeability of the formation, (mD)	0.01
Permeability of the fractured zone, (mD)	50000
Porosity of the formation, (%)	0.01
Porosity of the fractured zone, (%)	10
Water Saturation, (%)	100
Thermal conductivity of formation, (kJ/(m.day.C))	259
Thermal conductivity of water, (kJ/(m.day.C))	51.8
Volumetric heat capacity of the formation, (kJ/(m^3.C))	2130
Specific heat capacity of the fluid, (kJ/(kg.C))	4.82
Formation compressibility, (1/kPa)	4.40E-07
Temperature gradient, (C/m)	0.06
Reference depth, (m)	2500
Reference temperature, (C)	200

between the fluid and the reservoir is dominated by convection whereas the heat transfer within the reservoir is dominated by conduction (Fig. 3). As the rate of heat extraction in the reservoir is higher than the rate at which it replenishes itself, this results in decrease in the temperature of the reservoir, thus declining over time. In this study, no heat sources were considered to help replenish the reservoir but instead large enough reservoir was simulated to ensure that the boundaries of the reservoir remain unaffected even at the end of 30 years.

3.1. Temperature decline with different flow schemes

The flow rate of water circulated at a given time varies in each case and thus affects the heat extraction from the reservoir for the different flow schemes. Fig. 4 represents the variation in temperature decline curve when different flow schemes are used, keeping the injection temperature constant and the total fluid circulated per fracture is also kept constant (here Case 2 is used, the other two cases are described in the appendix).

As it can be inferred from Fig. 4, each scheme has a different decline curve for the temperature of produced water. This is because of the different flow rate for all the schemes at any given time hence the rate of heat transfer from reservoir to the circulating fluid also varies. Peak temperatures are attained at different times for the different flow schemes, and different end-point temperature at end of 30 years. But as the total amount of heat depends both on the temperature difference (between injected and produced fluid) and the flow rate, no conclusion can be drawn about their performance over time.

3.2. Cumulative heat

It would be better to get a combined result of different instantaneous flow rate and the instantaneous temperature of produced water. The total heat recovered could then be calculated for the various schemes from the produced water temperature profile and flow scheme. A typical temperature decline curve for the produced water when having a constant injection rate at constant temperature, is represented by Fig. 5. This can be used to calculate the instantaneous heat content of the produced water.

The instantaneous heat energy $\boldsymbol{h}(\boldsymbol{t})$, for the produced water can be calculated as shown in equation (12). Where, '$\boldsymbol{\rho}(\boldsymbol{T})$' represents the density of water which is a function of temperature [33], '$\boldsymbol{C_p}(\boldsymbol{T})$' represents the heat capacity of water which is also a function of temperature [34], $\boldsymbol{q}(\boldsymbol{t})$ represents the instantaneous flow rate (as per the flow scheme), $\boldsymbol{T}(\boldsymbol{t})$ represents the temperature of produced water and $\boldsymbol{T_{in}}$ represents the temperature of the injected water. The variation in heat capacity and density of water with temperature is shown in Fig. 6.

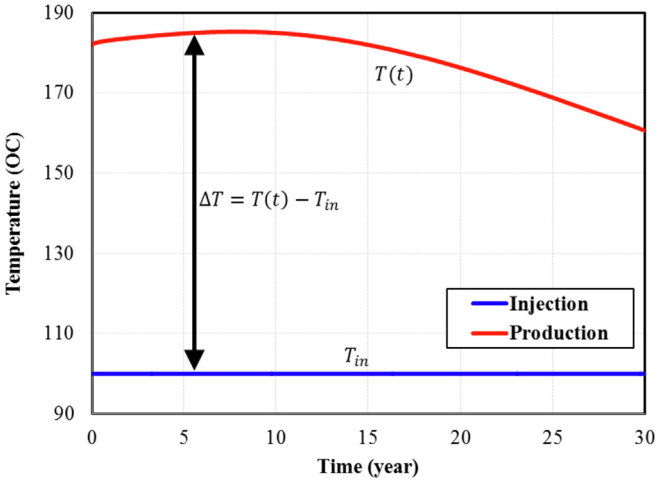

Fig. 5. Temperature decline curve in an EGS.

As the temperature of the produced water declines with time and the flow rate is constant, this indicates that there will be decline in power output also with time. Fig. 7 represents the cumulative heat produced by different flow schemes (keeping injection temperature same), which can be calculated by using equation (13) (here Case 2 is used, the other two cases are described in the appendix). The heat capacity and the density have opposite trends with respect to temperature above 50 ^{O}C, but the density is more strongly affected by the temperature (Fig. 6). For example, in case of constant flow rate, as the temperature of produced water 'T(t)' goes down, the density 'ρ(T)' increases. Because of the fact that the heat extraction is proportional to the heat capacity, density and temperature of the produced water, variations of these parameters in the opposite directions diminish the overall impact. In other words, this change in density compensates for the decline in temperature (and heat capacity) such that the instantaneous heat output remains constant over time and hence a linear cumulative heat output over the period of 30 years is obtained.

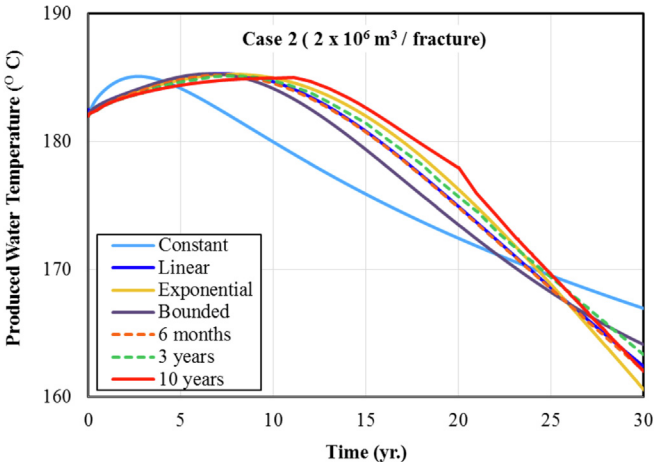

Fig. 4. Temperature decline curve with different flow scheme for Case 2.

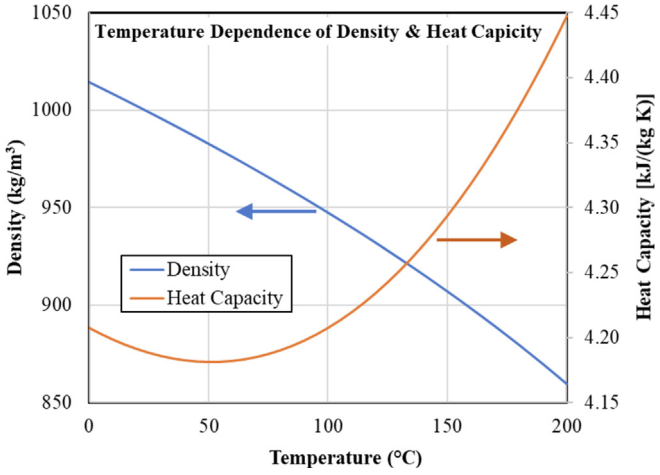

Fig. 6. Temperature dependency of heat capacity and density of water.

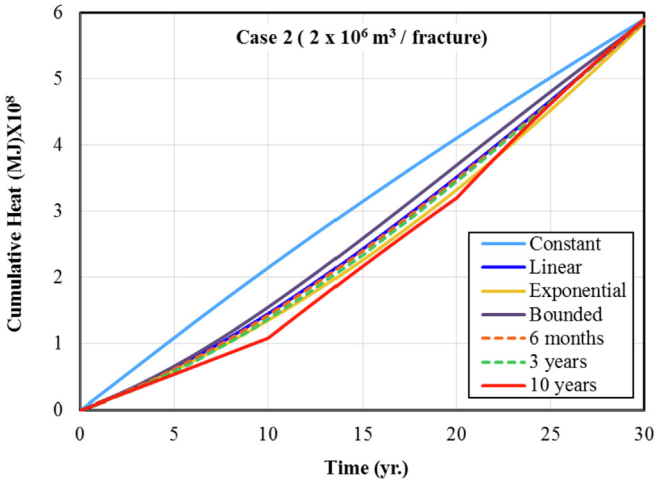

Fig. 7. Cumulative Heat extraction for different flow scheme with total flow represented in Q2.

$$\boldsymbol{h(t) = q(t).\rho(T).C_p(T).\Delta T = q(t).\rho(T).C_p(T).[T(t) - T_{in}]} \quad 12$$

$$H = \int_0^T h(t)dt \quad 13$$

For case 2, it was observed that each scheme results in a different rate of heat extraction with time, but the cumulative heat extracted in all the scheme at end of 30 years is same. This is due to the fact that the size of the reservoir is fixed and the total volume of fluid circulated is also constant in all the schemes. This shows that with systematic planning and operational optimization, different flow schemes can be used to produce heat as per our needs.

Fig. 8 represents the temperature profile for a cross section (y-z axis) of a single fracture along with position of injection and production wells. It can be observed that at initial condition different layers are set at different temperature, as per the geothermal gradient. At the end of 30 years, it was observed that all the profiles look very similar, confirming that the total amount of heat extracted over 30 years is almost constant in all the flow schemes. The minor differences in the total heat output for different flow schemes, arises from the varied heat transfer coefficients (dependent of flow rate and temperature) used in the simulator.

3.3. Instantaneous power

Instantaneous power is a better metric of EGS performance than cumulative heat extracted. The heat energy produced from the EGS can be used to run a power plant to provide power to a city/town. Depending on the temperature of the produced fluid and type of power plant, different methods are used to convert the thermal energy to electricity. Chamorro el. al. [35] talks about the different types of technologies used to convert the thermal energy to electricity, depending on the temperature and the phase of produced fluid. In this study a binary power plant was considered as most of the EGS are operated in a closed loop system to avoid water and pressure losses. A binary power plant usually consists of a different working fluid which is used to run the turbines to generate power. The produced fluid and the binary fluid never come in direct contact, rather a network of heat exchangers is used to transfer the heat from the produced fluid to the working fluid. Also, all of the heat produced by an EGS cannot be converted to electric power, due to the limitations of a binary power plant. This is why the efficiency of these plants are low, in general.

In a binary plant, the temperature of the produced fluid and flow rate of produced water are the two main factor that affect the efficiency of the power plant. This is an important consideration when calculating the sustainable and continuous power supply. An efficiency (***eff***) of 12% was used for the binary power plant to do the calculations. This is average efficiency calculated by Moon and Zarrouk [36] for binary power plants around the world. The instantaneous power for an EGS can be calculated as shown in equation (14). Where $\boldsymbol{P(t)}$ represents instantaneous power, $\boldsymbol{H(t)}$ represents instantaneous heat flow, $\boldsymbol{P(t)}$ represents the conversion efficiency of the binary power plant and $\boldsymbol{n_f}$ represents the total number of fractures. As all the fractures are considered to be identical and non-interactive, their output is additive.

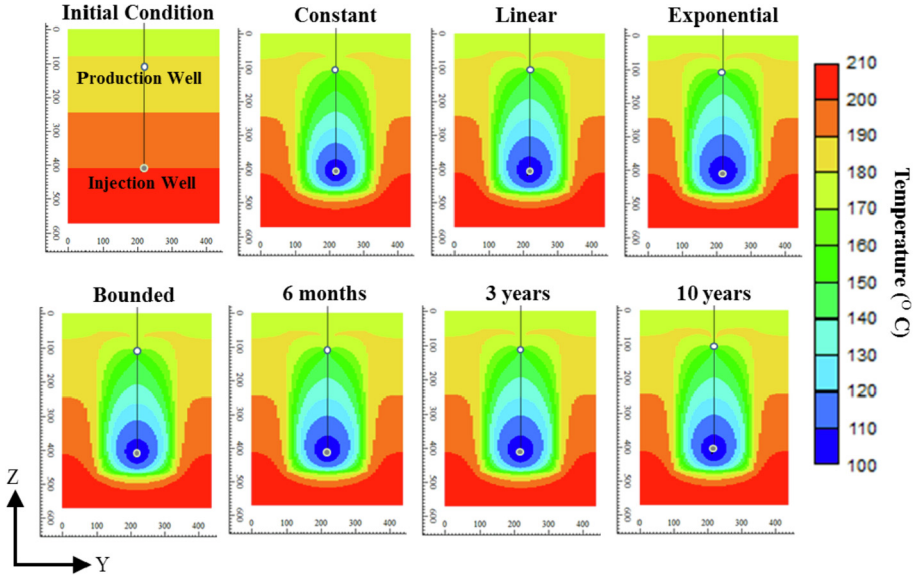

Fig. 8. Thermal profile of different flow schemes for case 2 at the end of 30 years.

$$P(t) = H(t) \times eff \times n_f \quad (14)$$

Using the instantaneous heat calculation from above sections, and assuming 50 fractures and the binary plant efficiency of 12%, the instantaneous power for different flow schemes can be calculated using equation (13). Fig. 9 shows the instantaneous power generated by different flow schemes for the total fluid flow of 2×10^6 $m^3/fracture$ over 30 years (here Case 2 is used, the other two cases are mentioned in appendix).

It was observed that each scheme has different power output at different time. The constant flow scheme has the highest power around 3.2 MW at the beginning, whereas all other scheme starts at 1.6 MW. This is because the constant flow scheme has the double flow rate than that of other schemes, extracting more heat and hence producing more power. The power output for the constant flow gradually decreases with time and is the lowest at the end of 30 years. In case of linear, and step flow (6 month, 3 year and 10 year), all of them start and end at the same point and is always increasing. This is because in step flow, even though the flow is increasing as per the step size, the growth is still linear in nature. In case of bounded exponential, the power output increase till a certain time, reaches it maximum and then starts to decline. This is because of the flow scheme itself. Initially the flow rate increases and then after a certain point it starts decreasing (see Fig. 3).

But, in case of exponential flow scheme, the power output increases almost linearly with time. As seen in Fig. 9, the power output starts at 1.6 MW and by the end of 30 years it gives the output of 4.2 MW, which is an increase of 62.5% over the entire time period. This proves to be an ideal situation when there is a need for increasing power output over time. This happens because the exponential flow has an exponentially growing flow rate that compensates for the decrease in average reservoir temperature with time. Though, in this flow scheme the heat is not produced at its maximum capability, this still works in our favor.

3.4. Effect of total flow

When the total amount of water injected per fracture is changed, it changes the temperature decline curve (see Fig. 10). It can be observed that keeping the injection temperature same, the three different total flow (Case 1, 2 and 3) results in three different decline curves, with lowest flow having highest temperature of produced water at the end of 30 years. This happens because when more water is circulated in the same amount of time, more amount of heat is extracted and the final temperature of the reservoir decreases [37].

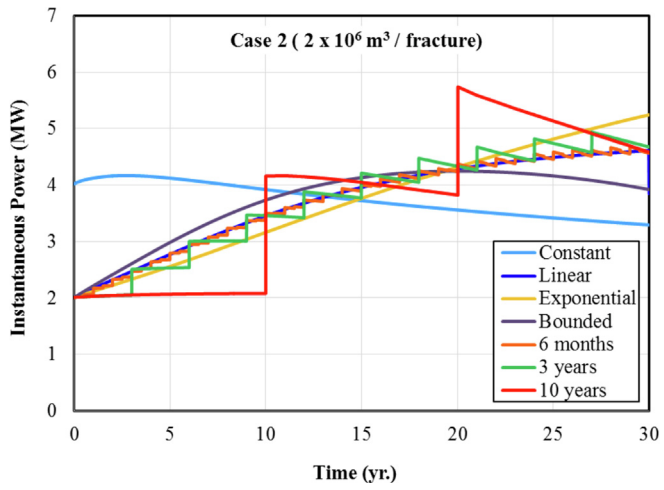

Fig. 9. Instantaneous power for different flow schemes.

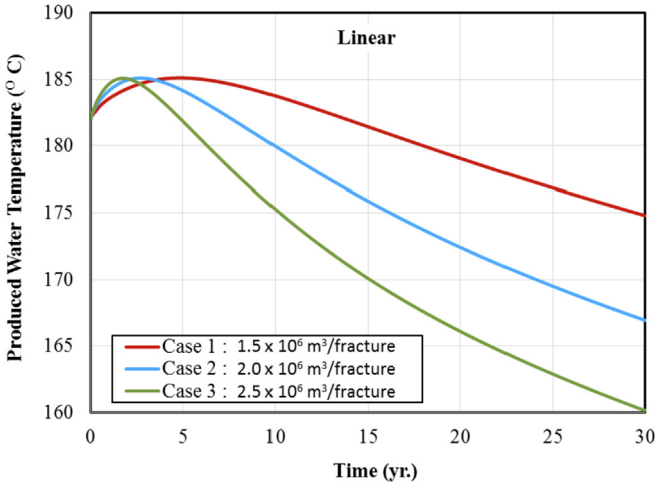

Fig. 10. Temperature decline curve with different amount of total flow.

Fig. 11 (a) shows the amount of cumulative heat extracted in three different cases along with different schemes. It shows that as the total amount of fluid that is circulated over 30 years, increase, the total amount of heat extracted is also increased. This is because the average temperature of the reservoir goes down further with increase in total flow. But having more fluid flow is not always the best case. Fig. 11 (b) shows the total amount of heat extracted per unit volume of fluid. It can be inferred that as the amount of total fluid increases, there is decrease in heat extracted per unit volume. This could lead to un-economic production of heat. Hence it is very important to find the right balance between cumulative heat and heat extracted per unit volume.

When building a power plant to meet the needs of a growing population, it is beneficial to account for the growth in power demand over time. Most of the simulations that have been carried out for EGS study have considered constant flow rate throughout its life, which proves not to be so effective because of its declining power output over time. As the reservoir size is fixed, it means there is a fixed amount of heat energy available for extraction. This indicates that when energy demand increases with, either the size of the reservoir needs to be increased or to build up another system, which would again be an expensive fleet. In this scenario, having an exponential flow scheme, proves to be beneficial to meet the energy demand of the growing city.

To ensure that the EGS would be able to keep up with the energy demand, there is a need to develop the EGS in a futuristic way by making it sufficiently large enough while planning and drilling. This way, using the exponential flow scheme, it would be able to match the energy demand with time and there would be no need to install another power plant. The biggest advantage of this scheme is that the power output can be controlled solely by the operational parameter (flow rate), making it flexible enough to increase or decrease the power output as needed.

4. Conclusions

This study focuses on the effect of different injection flow schemes that can be used to generate power from an EGS. Seven different flow schemes were evaluated in this study. All the other properties including the injection temperature and total amount of fluid circulated were kept constant.

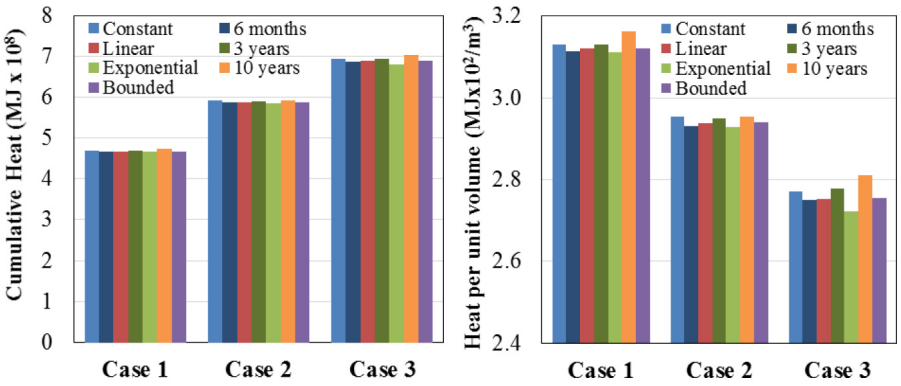

Fig. 11. (a) Cumulative heat extracted in three different cases, (b) Amount of heat extracted per unit volume of the fluid.

The temperature decline curves were different for all the different flow schemes reaching peak temperatures at different times. The cumulative heat calculated using the decline curves and the respective flow schemes showed that the total amount of heat extracted over 30 years was the same in all the cases. Instantaneous power output is a better criterion to compare the seven different flow schemes. Of the seven flow scenarios examined, the scheme where the flow rate is increased exponentially proved to be the best in terms of increasing power output over time. A linear growth in power of 62.5% was observed in the span of 30 years for the power output with this scheme. This type of power growth would be adequate to meet the increase of 48% energy demand in 30 years that the EIA has predicted. It is recognized that locally the growth in energy demand may be different.

It is also important to establish an optimum amount of fluid to be circulated over the time period, as increase in total fluid circulated leads to decrease in the amount of heat extracted per unit fluid volume making the process potentially uneconomic.

Successful implementation of EGS offers a potential to provide sustainable, renewable energy for decades. The optimization of one of the most important operational parameters (flow rate) would ensure generation of increased power over time to meet demand.

Acknowledgements

Authors acknowledge academic license to all of the reservoir simulation products developed by the Computer Modeling Group Limited (CMGL), Calgary, Canada.

Nomenclature

Symbol	*Description*	*Units*
$q(t)$	Instantaneous flow rate	m^3/day
a	Initial flow rate	m^3/day
b	Growth in flow rate	m^3/day
T	Total time period	*years*
C	Total amount of fluid circulated	m^3
n	Number of steps	
n_f	Number of fractures	
$h(t)$	Instantaneous heat	kJ/day
C_p	Specific heat capacity	$kJ/kg.°C$
ρ	Density of fluid	kg/m^3
ΔT	Temperature difference	$°C$
T_{in}	Temperature of injected fluid	$°C$
$T(t)$	Instantaneous temperature of produced fluid	$°C$
H	Total heat extracted over time	kJ
$P(t)$	Instantaneous Power	kW
eff	Efficiency of binary power plant	

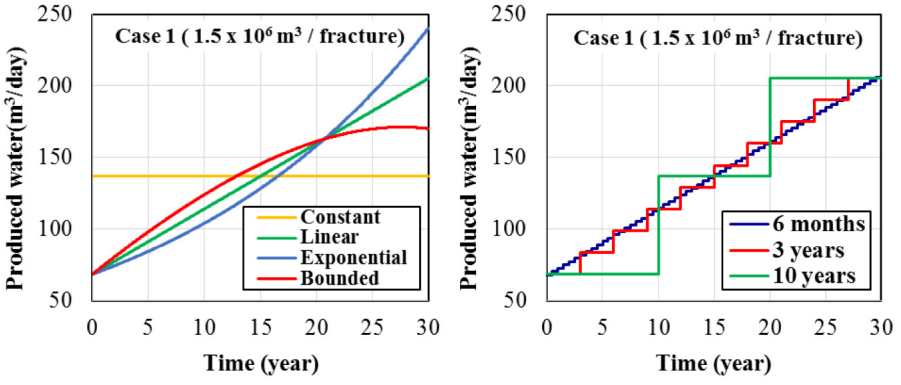

Fig. A.1. Instantaneous flow rate in each individual scheme for Case 1. (a) Flow scheme for continuous function, (b) Flow scheme for step functions.

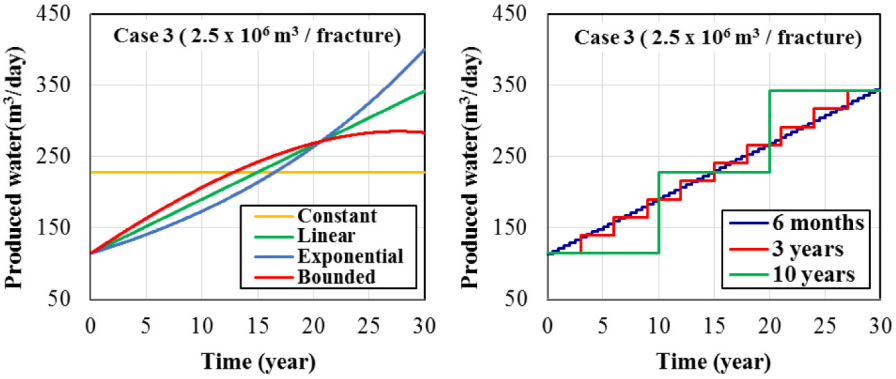

Fig. A.2. Instantaneous flow rate in each individual scheme for Case 3. (a) Flow scheme for continuous function, (b) Flow scheme for step functions.

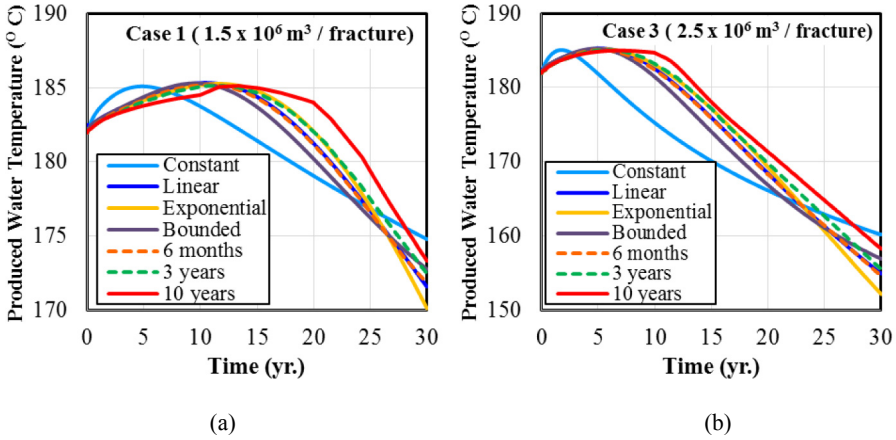

Fig. A.3. Temperature decline curve with different flow scheme for (a) Case 1 and (b) Case 3

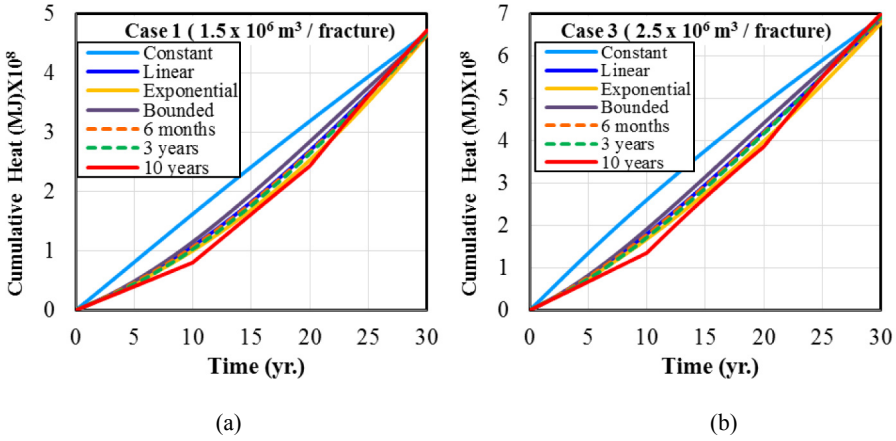

Fig. A.4. Cumulative Heat extraction for different flow scheme with total flow of (a) Case 1 and (b) Case 2.

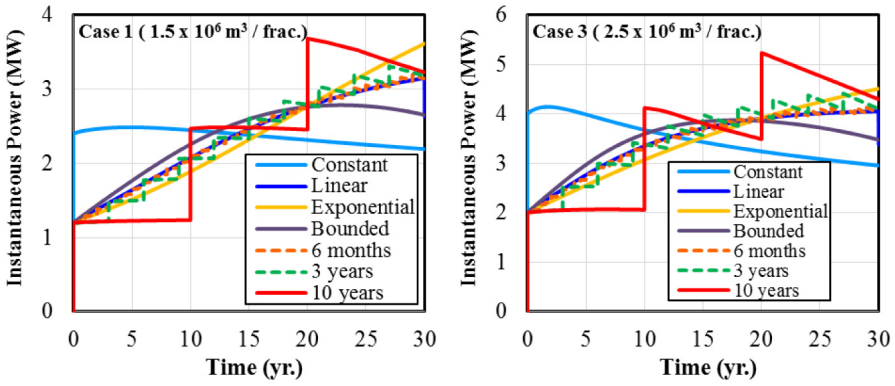

Fig. A.5. Instantaneous power output for different flow scheme with total flow of (a) Case 1 and (b) Case 2.

References

[1] Smith MC, Aamodt RL, Potter RM, Brown DW. Manmade geothermal reservoirs, LA-UR-75-953.CONF-750525-6. New Mexico, USA: Los Alamos Scientific Laboratory; 1975.

[2] Batchelor AS. The creation of Hot Dry Rock systems by combined explosive and hydraulic fracturing. In: Presented at the International conference on geothermal energy. Florence, Italy: BHRA Fluid Eng. Bedford; 1982.

[3] Tester JW, Brown DW, Potter RM. Hot dry rock geothermal energy – a new energy agenda for the 21st century, LA-11514-MS. New Mexico, USA: Los Alamos National Laboratory; 1989.

[4] Bataillé A, Genthon P, Rabinowicz M, Fritz B. Modeling the coupling between free and forced convection in a vertical permeable slot: implications for the heat production of an Enhanced Geothermal System. Geothermics 2006;35:654–82.

[5] D o. E. (DOE. An evaluation of enhanced geothermal systems technology. Geothermal Technologies Program; 2008.

[6] Li M, Lior N. Energy analysis for guiding the design of well systems of deep Enhanced Geothermal Systems. Energy 2015;93:1173–88.

[7] Wu B, Zhang X, Jeffrey RG, Bunger AP, Jia S. A simplified model for heat extraction by circulating fluid through a closed-loop multiple-fracture enhanced geothermal system. Appl Energy 2016;183:1664–81.

[8] Frash LP, Gutierrez M, Hampton J, Hood J. Laboratory simulation of binary and triple well EGS in large granite blocks using AE events for drilling guidance. Geothermics 2015;55:1–15.

[9] Chen J, Jiang F. Designing multi-well layout for enhanced geothermal system to better exploit hot dry rock geothermal energy. Renew Energy 2015;74:37–48.

[10] Pandey SN, Vishal V. Sensitivity analysis of coupled processes and parameters on the performance of enhanced geothermal systems. Sci Rep Dec 6 2017;7:17057.

[11] Pandey SN, Chaudhuri A, Kelkar S. A coupled thermo-hydro-mechanical modeling of fracture aperture alteration and reservoir deformation during heat extraction from a geothermal reservoir. Geothermics 2017;65:17–31.

[12] Gholizadeh Doonechaly N, Abdel Azim RR, Rahman SS. A study of permeability changes due to cold fluid circulation in fractured geothermal reservoirs. Gr Water May 2016;54:325–35.

[13] Vazquez-Rubio IG, Bahrami D, Danko G. Numerical simulation model comparisons for enhanced geothermal reservoirs. Trans Geoth Resour Counc 2015;39.

[14] Sanyal SK, Butler SJ. An Analysis of power generation prospects from enhanced geothermal system. In: Proceedings World geothermal congress; 2005. 24-29 April, Antalya, Turkey.

[15] Aliyu MD, Chen H-P. Sensitivity analysis of deep geothermal reservoir: effect of reservoir parameters on production temperature. Energy 2017;129:101–13.

[16] Sun Z-x, Zhang X, Xu Y, Yao J, Wang H-x, Lv S, et al. Numerical simulation of the heat extraction in EGS with thermal-hydraulic-mechanical coupling method based on discrete fractures model. Energy 2017;120:20–33.

[17] Xia Y, Plummer M, Mattson E, Podgorney R, Ghassemi A. Design, modeling, and evaluation of a doublet heat extraction model in enhanced geothermal systems. Renew Energy 2017;105:232–47.

[18] Zeng Y-C, Wu N-Y, Su Z, Wang X-X, Hu J. Numerical simulation of heat production potential from hot dry rock by water circulating through a novel single vertical fracture at Desert Peak geothermal field. Energy 2013;63:268–82.

[19] Asai P, Panja P, McLennan J, Moore J. Performance evaluation of enhanced geothermal system (EGS): surrogate models, sensitivity study and ranking key parameters. Renew Energy 2018;122:184–95.

[20] 2018 06/01). https://www.eia.gov/todayinenergy/detail.php?id=26212..

[21] Pandey SN, Chaudhuri A, Rajaram H, Kelkar S. Fracture transmissivity evolution due to silica dissolution/precipitation during geothermal heat extraction. Geothermics 2015;57:111–26.

[22] Guo B, Fu P, Hao Y, Peters CA, Carrigan CR. Thermal drawdown-induced flow channeling in a single fracture in EGS. Geothermics 2016;61:46–62.

[23] Luo J, Zhu Y, Guo Q, Tan L, Zhuang Y, Liu M, et al. Chemical stimulation on the hydraulic properties of artificially fractured granite for enhanced geothermal system. Energy 2018;142:754–64.

[24] Asai P, Panja P, McLennan J, Moore J. Efficient simulation and modeling of multifractured enhanced geothermal systems (EGS). Renew Energy 2019;131:763–77.

[25] Shook GM, Suzuki A. Use of tracers and temperature to estimate fracture surface area for EGS reservoirs. Geothermics 2017;67:40–7.

[26] McDermott CI, Randriamanjatosoa ARL, Tenzer H, Kolditz O. Simulation of heat extraction from crystalline rocks: the influence of coupled processes on differential reservoir cooling. Geothermics 2006;35:321–44.

[27] Gwynn M, Allis R, Hardwick CL, Hill J, Moore J. A new look at the thermal regime around roosevelt hot spring. In: 41st workshop on geothermal reservoir engineering. Stanford, CA: Stanford University; 2016.

[28] Simmons S, Kirby S, Jones C, Moore J, Allis R. The geology, geochemistry, and hydrology of the EGS FORGE site, Milford Utah. In: 41st workshop on geothermal reservoir engineering. Stanford, CA: Stanford University; 2016.

[29] (2018 6/1/2018). http://www.forgeutah.com/site/

[30] Hofmann H, Weides S, Babadagli T, Zimmermann G, Moeck I, Majorowicz J, et al. Potential for enhanced geothermal systems in Alberta, Canada. Energy 2014;69:578–91.

[31] Ansari E, Hughes R, White CD. Statistical modeling of geopressured geothermal reservoirs. Comput Geosci 2017;103:36–50.

[32] Ansari E, Hughes R, White CD. Modeling a new design for extracting energy from geopressured geothermal reservoirs. Geothermics 2018;71:339–56.

[33] DDBST. Dortmund data bank software & separation technology GmbH: saturated liquid density. 2019. Available: http://ddbonline.ddbst.de/DIPPR105DensityCalculation/DIPPR105CalculationCGI.exe.

[34] The engineering ToolBox: water - heat capacity (specific heat). Available: https://www.engineeringtoolbox.com/specific-heat-capacity-water-d_660.html.

[35] Chamorro CR, Mondéjar ME, Ramos R, Segovia JJ, Martín MC, Villamañán MA. World geothermal power production status: energy, environmental and economic study of high enthalpy technologies. Energy 2012;42:10–8.

[36] Zarrouk SJ, Moon H. Efficiency of geothermal power plants: a worldwide review. Geothermics 2014;51:142–53.

[37] Shaik AR, Rahman SS, Tran NH, Tran T. Numerical simulation of Fluid-Rock coupling heat transfer in naturally fractured geothermal system. Appl Therm Eng 2011;31:1600–6.